

Navigating Data Corruption in Machine Learning: Balancing Quality, Quantity, and Imputation Strategies

Qi Liu¹ and Wanjing Ma²

^{1,2}College of transportation engineering, Tongji University, Shanghai, P.R.China,
201804

{liu.qi, mawanjing}@tongji.edu.cn

December 25, 2024

Abstract

Data corruption, including missing and noisy data, is an inevitable challenge in real-world machine learning applications. This paper investigates the impact of data corruption on model performance and explores strategies to mitigate its effects through two distinct experimental setups: supervised learning with NLP tasks (NLP-SL) and deep reinforcement learning for traffic signal optimization (Signal-RL). We evaluate the relationship between data corruption levels and model performance, assess the effectiveness of various data imputation methods, and analyze the utility of enlarging datasets to offset data corruption.

Our findings reveal that model performance under data corruption follows a diminishing return curve, well-modeled by the exponential function $S = a(1 - e^{-b(1-p)})$, where p is the corruption ratio. Missing data, while harmful, is less detrimental than noisy data, which causes rapid performance degradation and increased training instability, particularly in sequential decision-making tasks like Signal-RL. Imputation strategies introduce a trade-off between recovering missing information and introducing noise, with their effectiveness heavily dependent on imputation accuracy and corruption ratio. We identify a distinct “imputation advantageous corner” and “imputation disadvantageous edge” on an imputation advantage heatmap, and categorize tasks as either “noise-sensitive” or “noise-insensitive” based on their imputation decision boundaries.

Additionally, we show that increasing the dataset size mitigates, but does not fully eliminate, the effects of data corruption, especially under high noise levels. The marginal utility of additional data diminishes as corruption levels increase, confirming the exponential nature of the trade-off between data quality and quantity. An empirical rule emerges from our study: approximately 30% of the data is critical for determining model performance, while the remaining 70% has a minimal impact.

These findings provide practical insights into data preprocessing, imputation strategy selection, and resource allocation for data collection, offering actionable guidance for building robust machine learning systems in noisy, real-world environments.

1 Introduction

The advent of large language models (LLMs), such as GPT-3 and BERT, has revolutionized natural language processing (NLP), enabling machines to understand and generate human-like text with remarkable proficiency. Pre-training these models requires vast amounts of data to capture the nuances and complexities of human language. However, real-world datasets are often riddled with corrupted data, which can significantly impede the performance of LLMs if not properly addressed. Handling corrupted data is, therefore, a critical step in the pre-training pipeline, necessitating robust methods to ensure data integrity and model efficacy.

Corrupted data can arise from various sources, such as transmission errors or incomplete data collection processes. Data corruption manifests in different forms, including missing data and noisy data. The presence of corrupted data poses serious challenges to a model’s learning ability. Consequently, employing effective strategies to handle corrupted data is essential to maximize the potential of LLMs.

While numerous data imputation methods exist, their effectiveness in enhancing neural network learning efficiency remains unclear. LLMs have the inherent capability to learn directly from corrupted data, albeit at reduced efficiency. This raises important questions: What is the relationship between data corruption percentage and model performance? Can the “brute force” approach of adding more data compensate for poor data quality? If so, how much additional effort is required?

In this work, we explore the behavior of deep learning models under varying levels and types of data corruption. We conduct experiments on two types of tasks: supervised learning (NLP-SL) and reinforcement learning (Signal-RL). Additionally, we study the effectiveness of data imputation methods by comparing them against a no-imputation baseline. This study seeks to answer whether enlarging the dataset can mitigate the degradation caused by noise and, if so, how much additional data is needed. The insights gained from this study aim to provide guidance for data collection and preprocessing strategies.

The key takeaways from this paper may be summarized as follows:

1. **Diminishing Returns in Data Quality Improvement:** Improving data quality has diminishing returns on model performance. The relationship between the model score S and noise level p is well-modeled by the function:

$$S = a(1 - e^{-b(1-p)})$$

where parameter $a = \frac{S_0}{1-e^{-b}}$; and S_0 is the model score when $p = 0$ (i.e., no corruption).

2. **Data Noise is More Detrimental than Missing Data:** Noise causes more severe performance degradation compared to missing data. It also contributes to training instability, making the learning process less reliable.
3. **Trade-offs in Data Imputation:** Imputing missing data can introduce noise, resulting in a trade-off. The imputation advantage heatmap highlights two key regions:
 - Imputation Advantageous Corner: A region where accurate imputation significantly boosts model performance.
 - Imputation Disadvantageous Edge: A region where imputation noise outweighs its benefits, harming model performance.
4. **Two Types of Tasks Identified:** Tasks are classified into two categories based on their sensitivity to noise:
 - Noise-insensitive tasks: These tasks exhibit gradual performance degradation and are characterized by a decision boundary on the heatmap fitted by a sigmoid curve.
 - Noise-sensitive tasks: These tasks show sharp performance declines, with decision boundaries well-modeled by an exponential curve.
5. **Limits of Enlarging Datasets:** Data corruption leads to performance declines that cannot be fully recovered by simply increasing the sample size. Enlarging datasets does not entirely offset the detrimental effects of corruption.
6. **Impact of Noise on Learning Efficiency:** Data noise hampers learning efficiency. To achieve the same performance level (if at all possible), the number of required samples—and hence training time—increases exponentially with the noise level.
7. **Empirical Rule on Data Importance:** Approximately 30% of the data is critical for determining model performance, while the remaining 70% can be lost with minimal impact on performance. This finding provides practical guidance for data collection and prioritization.

2 Related Work

Types of Data Corruption

Data corruption in machine learning encompasses various forms, including missing data, noisy data, and adversarial perturbations. This study focuses on two major types of corruption: missing data and noisy data, which commonly occur in real-world scenarios.

Missing Data: Missing data can result from sensor dropout, incomplete data collection, or non-response in surveys. Rubin’s classification categorizes missing data into three types: Missing Completely at Random (MCAR), Missing at Random (MAR), and Missing Not at Random (MNAR) [Rub76]. In NLP, missing data often manifests as masked or unknown tokens, while in reinforcement learning, it appears as incomplete state observations.

Noisy Data: Data noise can affect both labels and features, with sources ranging from environmental factors to measurement errors. Noise is often categorized by its statistical distribution (e.g., Gaussian, uniform) or type (e.g., additive, multiplicative). Noisy data significantly disrupts model learning, particularly when noise affects key features or labels critical to decision-making.

Handling Corrupted Data

Data imputation aims to recover missing information, and various strategies have been proposed: • **Statistical Methods:** These include simple approaches like mean, mode, or median imputation [SG02], as well as more sophisticated techniques like regression imputation and multiple imputation [Rub87]. While straightforward, these methods may introduce bias or underestimate variability. • **Machine Learning Methods:** Techniques such as K-Nearest Neighbors (KNN) imputation [TCS+01], decision tree-based imputation [BFOS84], and Random Forest imputation [Bre01] leverage patterns in data to predict missing values. • **Deep Learning-Based Imputation:** Autoencoders and Generative Adversarial Networks (GANs) have emerged as powerful tools for data imputation. Denoising autoencoders reconstruct inputs with missing values [VLBM08], while GANs generate plausible synthetic data to fill gaps [GPAM+14]. Yuan et al. (2021) used masked language models (e.g., BERT) to impute missing tokens in text data [YWZ21].

For many applications, particularly LLM pre-training, masking missing data is often sufficient. Che et al. (2018) showed that masking missing time-series data combined with recurrent neural networks (e.g., GRU) can effectively handle missingness [CPC+18].

Impact of Data Corruption on Neural Network Learning

Supervised Learning (LLM Pre-training) Data corruption, including missing or noisy tokens, can significantly impair pre-trained language models like BERT and GPT. Missing data reduces the available context, weakening learned representations and hindering downstream tasks such as summarization or question answering [Dev18, Liu19]. Joshi et al. (2020) showed that missing rare tokens during pre-training leads to incomplete token embeddings, limiting the model’s ability to capture fine-grained semantics [JCL+20].

Noisy data, particularly in large-scale corpora, introduces biases and degrades model robustness. Brown et al. (2020) highlighted that noisy training data increases the likelihood of generating biased or low-quality outputs, while filtering and robust training objectives mitigate such effects [Bro20]. Semantic noise, such as contradictory or irrelevant text, reduces the model’s ability to retain factual knowledge and generalize across tasks [PPF+20]. Studies by Gehman et al. (2020) further demonstrated that noisy datasets amplify harmful biases, underscoring the importance of pre-training data quality [GGs+20].

Reinforcement Learning In reinforcement learning (RL), data corruption affects state observations, which are critical for decision-making. Missing features reduce state informativeness, leading to suboptimal policies, particularly in partially observable environments (POMDPs) [HS15]. Studies by Bai et al. (2021) demonstrated that missing features disrupt state transition dynamics, causing instability in model-free RL algorithms and inaccurate environment models in model-based RL [BGW19].

Noise in feature data further degrades RL performance. Pathak et al. (2017) showed that noisy features distort latent state representations, leading to poor decision-making in high-dimensional environments [PAED17]. Mnih et al. (2015) found that Q-values fluctuate with noisy observations, resulting in unstable policies [MKS+15]. Moreover, noise hampers transfer learning, as policies trained in corrupted environments fail to generalize to clean environments [TS09].

Key Research Gaps

While many studies address specific aspects of corrupted data handling, key questions remain unanswered:

- **Impact of Data Corruption:** What is the quantitative relationship between data corruption ratio and model performance? Can this relationship be consistently modeled across tasks?
- **Effectiveness of Imputation:** How do different imputation methods compare in mitigating the effects of missing data? Is it possible to fully restore the utility of corrupted data through imputation?

- Trade-Off Between Data Quality and Quantity: Can larger datasets compensate for data corruption? How much additional data is required to offset quality issues, and does the marginal utility of additional data diminish with increasing corruption?

This study aims to bridge the above gaps by evaluating the effects of data corruption on supervised and reinforcement learning tasks. We explore the utility of data imputation methods and analyze the trade-off between data quality and quantity, providing insights to guide data collection and preprocessing strategies.

3 Learning with corrupted data

Experiment Design

We designed two experiments, NLP supervised learning (NLP-SL) and traffic signal deep reinforcement learning (Signal-RL), to investigate the impact of data corruption. These two vastly different experimental setups were chosen because the questions we aim to explore are general and relevant across a wide range of machine learning tasks. By selecting tasks that are diverse in nature, we hope to derive more general insights and uncover deeper connections between these seemingly unrelated domains.

The first experiment focuses on the GLUE benchmark tasks. We use the pretrained [BERT](#) model as the base model and add feedforward layers on top to fine-tune it on eight tasks: CoLA, SST-2, MRPC, STSB, QQP, MNLI, QNLI, and RTE. The input data is corrupted by replacing certain words with the “[UNK]” token, while the labels y remain uncorrupted. This type of data corruption is commonly encountered in natural language processing tasks. For instance, when digitizing text corpora, some words may become indistinguishable and are thus masked as unknown, whereas the associated labels are typically unaffected. Evaluating the amount of knowledge learned by a model remains a subjective challenge. In this experiment, we measure performance using classification-related accuracy metrics. Specifically:

- The Matthews Correlation Coefficient (MCC) is used for CoLA.
- The average of Pearson and Spearman correlation coefficients is used for STSB.
- Test accuracy is used for the remaining tasks.

Baseline scores (1/2 for binary classification and 1/3 for three-way classification) are subtracted from these metrics. The final model score is calculated as the average of the scores across all tasks. To ensure consistency, hyperparameters such as training epochs and learning rates are tuned using uncorrupted data and kept fixed for all subsequent experiments. Model convergence for these experiments is illustrated in Figure 2. For the sake of clarity, we will refer to this experiment as the “Natural Language Processing - Supervised Learning (NLP-SL)” experiment in the following sections.

The second experiment is a deep reinforcement learning (RL) task. We built an isolated intersection environment using SUMO. The environment is illustrated in Figure 1. The objective is to optimize the traffic signal at this intersection. The intersection consists of four approaches, each with three lanes. The traffic demand is generated using a binomial distribution, and the ratio of left-turn, through, and right-turn traffic demands is 1:3:2. The arrival rates are time-varying: East-West traffic demands follow a sine curve, while North-South demands follow a cosine curve, both within the interval $[0, \pi/2]$. The time horizon H for the simulation is one hour.

A Deep Q-Network (DQN) model is used to learn the traffic signal control strategy. The state of the environment consists of road occupancy, the current signal phase, and the duration of the current signal phase, resulting in a state vector of dimension 965. A neural network with two hidden layers of sizes 256 and 48 is used to extract features. Layer normalization is applied, but no dropout layers are included. Standard techniques such as double networks and replay buffers are implemented. The action space is discrete, with four possible actions: East-West left turn, East-West through, North-South left turn, and North-South through. Each time step in the simulation corresponds to 6s. The reward r_t for each time step is defined as the queuing vehicles’ value transformed according to Equation 1. The performance metric for the model is the episode cumulative reward, R . Although the reward is accumulated over one hour, the process itself is infinite.

$$R = \sum_{t=1}^H r_t = \sum_{t=1}^H -\frac{q_t - 80}{80} \quad (1)$$

where q_t is the number of queuing vehicles at time t ; and the threshold for deciding whether a vehicle is stopped is $0.3m/s$.

We trained the model using linearly decaying exploration (ϵ) and learning rate (lr) for 80% of the training time, after which the values were fixed. The initial and final ϵ values were 1.0 and 0.01, respectively, while the initial and final learning rates were $1e-3$ and $1e-4$, respectively. The DQN model convergence results are shown in Figure 2(b).

We experimented with three types of data corruption: vehicle-missing, inserting-noise, and masking-region:

1. Vehicle-missing: A proportion of the vehicles are not detected. This scenario is relevant in Vehicle-to-Everything (V2X) environments, where roadside units detect vehicles’ presence through communication channels like DSRC [THBM19]. However, only a proportion of vehicles are equipped with onboard devices. This type of corruption is analogous to the data missing scenario in the NLP-SL experiment.
2. Inserting-noise: Noise is added to the road occupancy state and rewards. This scenario is relevant in environments where vehicles are detected using computer vision systems, which can introduce errors.
3. Masking-region: This special type of corruption is specific to traffic signal settings. The simulation environment assumes a lane length of 400 meters. A masking-region ratio p means that the farthest $400 \cdot p$ meters of each lane will be invisible to the model, simulating the range limitations of video cameras used for vehicle detection.

Observations

Figure 4 illustrates the relationship between the data missing ratio and model performance. Both experiments (NLP-SL and Signal-RL) show a gradual initial decline in performance, followed by a steeper descent, culminating in a sharp drop-off as the data missing ratio approaches 1.0. For reference, we include the performance of an optimized fixed-timing signal as a benchmark in the figure. The RL-trained signal outperforms the fixed-timing signal when the data missing ratio is less than 0.8.

Tables 1 and 2 provide the detailed data for these experiments. In Figure 5, we change the x-axis to represent $1 - \text{corruption ratio}$ and fit the curve to the function in Equation 1. The fitted parameters for the NLP-SL experiment are: $a = 0.475$, $b = 3.517$, where b represents the decay rate that controls the curve’s steepness. The goodness-of-fit analysis results in $R^2 = 0.995$, indicating that the exponential cumulative distribution function (CDF) is an excellent model for the observed performance. Similarly, for the Signal-RL experiment, the fitted curve parameters are: $a = 395.827$, $b = 7.493$ with $R^2 = 0.956$.

This striking coincidence reveals an important and universal rule in machine learning: the diminishing return of data. The decay rate b reflects the task’s nature, with the RL task demonstrating a much larger decay rate. This implies that RL tasks are more sensitive to noise compared to NLP tasks.

$$S = a(1 - e^{-b(1-p)}) \quad (2)$$

where parameter $a = \frac{S_0}{1 - e^{-b}}$; and S_0 is the model score when $p = 0$ (i.e., no corruption).

Here, we provide an explanation for the observed pattern. For both NLP and DRL tasks, the model relies on recognizing patterns (e.g., semantic patterns, queuing patterns) in the data. When the data is completely corrupted, the critical patterns necessary for performance are entirely lost. As corruption decreases, the model rapidly recovers key patterns, resulting in a steep improvement in performance. However, once most of the critical patterns have been recovered, the marginal utility of additional clean data diminishes, leading to a saturation of performance.

As we know, the probabilities of observing rare events over a large number of trials converge to the Poisson distribution. When n (the number of trials) is large, p' (the probability of success per trial) is small, and the expected number of successes $\lambda = n \cdot p'$ is finite, the binomial distribution approximates the Poisson distribution:

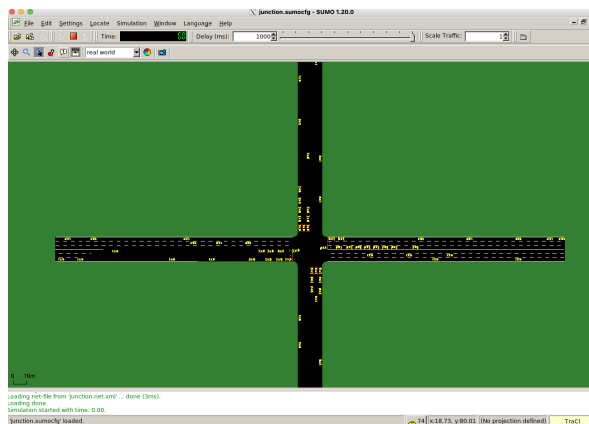


Figure 1: Isolated intersection simulation environment (SUMO)

$$P(K = k) \approx \frac{\lambda^k e^{-\lambda}}{k!}, \quad (3)$$

where $\lambda = n \cdot p'$ is the rate parameter, representing the expected number of successes.

The exponential term $e^{-\lambda}$ in the Poisson distribution describes the probability of observing 0 successes, or equivalently, the probability of failure. In both experiments, the dataset size n is large, making the recovery of individual patterns a rare event that can be modeled using the Poisson distribution. In our experiments, each pattern has an equal probability p of being corrupted, or a probability $x = 1 - p$ of being recovered. A pattern can be recovered multiple times in the dataset. The probability of failing to recover such a pattern in a dataset with corruption level p is proportional to e^{-x} . This leads to a system where the rate of change in performance depends on the difference between the system’s current state and its limit. Such behavior can be modeled using Equation 4, whose solution corresponds to Equation 1:

$$\frac{dS}{dx} = abe^{-bx} = b(a - S) \quad (4)$$

where $x = 1 - p$.

This model effectively explains the exponential improvement observed in performance as corruption decreases and clean data proportion increases.

The Signal-RL model scores under inserting-noise and masking-region types of data corruption are shown in Figure 6. From Figure 6(a), we observe that inserting noise is significantly more detrimental than data-missing. The model’s performance deteriorates much more rapidly as the noise level increases, falling below the fixed-timing signal performance as soon as the noise level exceeds 10%. Additionally, the model scores become unstable, as indicated by the oscillations in Figure 6(a). The training process also becomes unstable, as shown in Figure 7.

Masking-region is a unique type of data-missing corruption. Information about vehicles farther away from the intersection is less critical. By gradually discarding less important data, we observe that the model score only experiences a sharp decline when the masking ratio p exceeds 0.7. This observation leads to an empirical rule: 30% of the data is critical and determines the model’s performance, while the remaining 70% can be discarded without significantly affecting the model’s performance.

4 Effectiveness of Data Imputation

In this section, we assess whether and how different imputation strategies mitigate the impact of missing data. We note that the decision on whether to impute missing data involves a trade-off between data-missing and noise-inserting. We distinguish two common types of data-missing scenarios often encountered in practice:

1. The first type occurs when the exact location of missing data is known. This is typical for NLP tasks, where missing words are marked with tokens like “[UNK].”

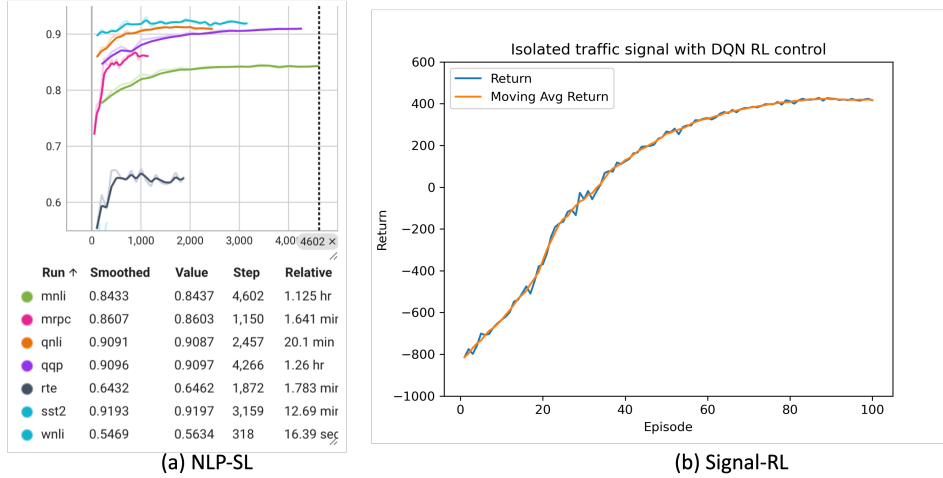


Figure 2: Model convergence of two experiments. (a) NLP-SL experiment (b) Signal-RL experiment

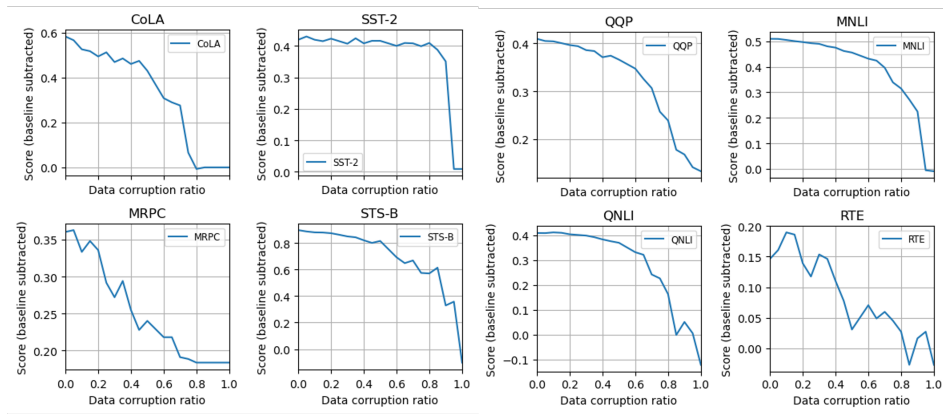


Figure 3: NLP-SL model performances under different data corruption ratios. Most tasks exhibit Equation 1 pattern except MRPC and RTE tasks.

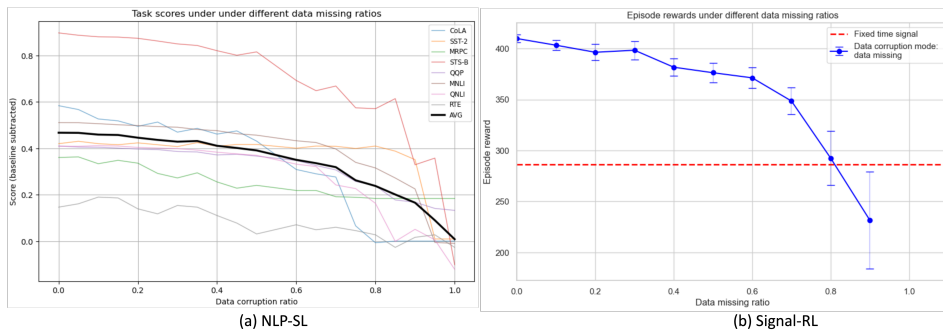


Figure 4: Model performances under different data corruption ratios (a) NLP-SL experiment. (b) Signal-RL experiment.

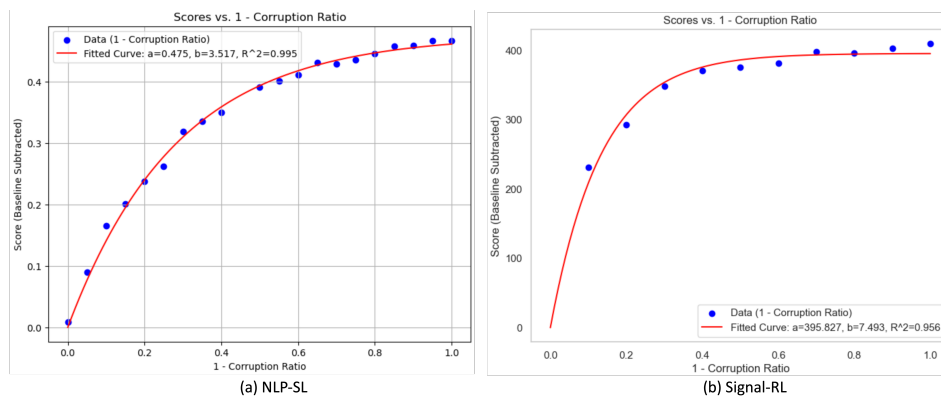


Figure 5: The relationship between model learning and data corruption ratio fitted by Equation 1; X-axis is 1 - data corruption ratio. (a) NLP-SL experiment. (b) Signal-RL experiment. Both experiments exhibit diminishing returns when data quality improves.

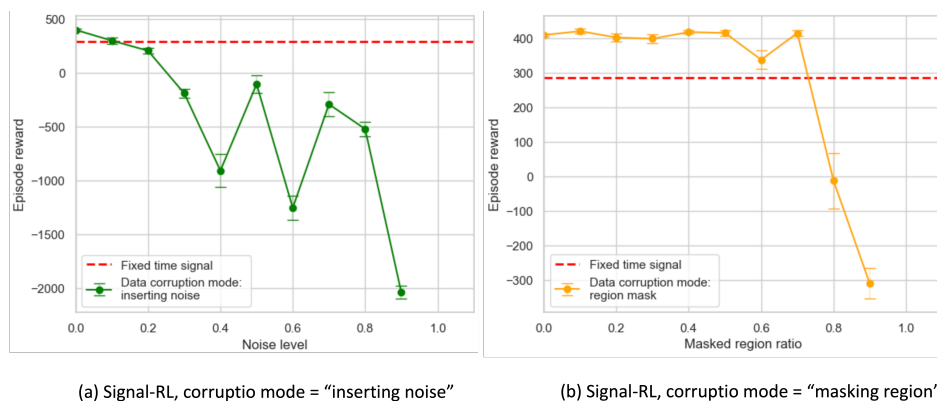


Figure 6: Signal-RL model performance under varying data corruption ratios (a) corruption mode = inserting noise. Inserting noise is more detrimental than data missing; and model performance becomes unstable. (b) corruption mode = masking region. Model performance does not degrade when 70% less important data are lost.

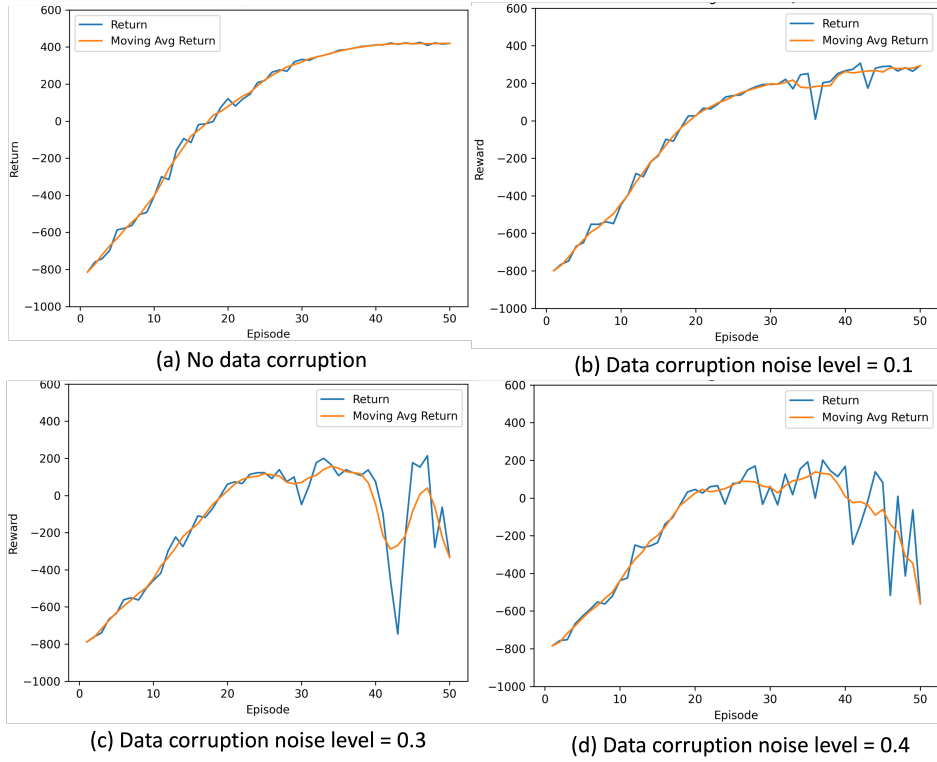


Figure 7: Training process becomes unstable when corruption mode is inserting noise

Data missing ratio	0.0	0.05	0.1	0.15	0.2
Model score	0.4669	0.4663	0.4588	0.4572	0.4455
Data missing ratio	0.25	0.3	0.35	0.4	0.45
Model score	0.4359	0.4283	0.4312	0.4106	0.4012
Data missing ratio	0.5	0.6	0.65	0.7	0.75
Model score	0.3906	0.3501	0.3357	0.3186	0.2619
Data missing ratio	0.8	0.85	0.9	0.95	1.0
Model score	0.2375	0.2008	0.1654	0.0897	0.0081

Table 1: NLP-SL model scores at different data missing ratios.

Data missing ratio	0.0	0.1	0.2	0.3	0.4
Model score mean	409.86	403.30	396.40	398.40	381.74
Model score std	3.83	5.04	7.92	8.97	8.44
Data missing ratio	0.5	0.6	0.7	0.8	0.9
Model score mean	376.33	371.30	348.58	292.54	231.56
Model score std	9.62	10.05	13.25	26.44	47.59

Table 2: Mean and standard deviation of Signal-RL model scores at different data missing ratios.

- The second type occurs when the location of missing data is not known. For example, in the Signal-RL experiment, vehicles are sometimes not detected, and we do not know which elements of the state vector are corrupted. To impute data in this second scenario, every possible location must be checked, which introduces significantly more noise than in the first case.

We will refer to these two scenarios as “exact imputation” and “general imputation,” respectively.

Experiment Design

We experiment with these imputation methods under varying data-missing ratios. There are various

types of imputation methods, as reviewed in the literature. However, evaluating the effectiveness of these algorithms is non-trivial, and their accuracies are not adjustable parameters. For our study, where we focus on the trade-off between data-missing and noise, it is crucial to control the accuracy of imputation. To achieve this, we propose using an “inserting-noise” imputation method. In this method, accurate words (for NLP-SL) or state elements (for Signal-RL) are randomly replaced with random values, allowing us to control the imputation noise level, denoted as q . Later, we also experiment with traditional imputation methods and evaluate their effectiveness.

Let $S(p)$ represent the model score when the data-missing ratio is p and no imputation is applied. Let $\tilde{S}(p, q)$ represent the model score when the data-missing ratio is p and an imputation method with noise level q is used to preprocess the data before training. We define the imputation advantage, $A(p, q)$, as:

$$A(p, q) = \tilde{S}(p, q) - S(p) \tag{5}$$

$A(p, q)$ quantifies the improvement (or harm) caused by imputation relative to no imputation. Figure 8 shows the heatmap of imputation advantage for both experiments.

Observations

Several interesting observations can be made from the heatmaps. First, the Signal-RL task is much more sensitive to imputation noise, primarily because it involves general imputation. Red regions on the heatmap indicate areas where imputation is beneficial, while blue regions indicate areas where imputation harms model performance. The heatmaps clearly demonstrate the trade-off between data-missing and noise, and we identify two distinct regions:

1. Red Corner: This region is located in the lower right corner of the heatmap, where the data-missing ratio is high, and the imputation noise level is low. Accurate imputation in this region restores critical information, leading to significant improvements in model performance.
2. Blue Edge: This region is near the edge where $q = 1$. When the imputation noise level approaches 1.0, the noise introduced during imputation overwhelms the model, leading to performance degradation. Interestingly, the greatest harm occurs when the data-missing ratio is around $p = 0.6$.

Additionally, we draw the contour line corresponding to $A(p, q) = 0$ on the heatmap. This line represents the decision boundary between the imputation-advantageous and imputation-disadvantageous regions. A few notable differences between the Signal-RL and NLP-SL tasks can be observed:

1. Signal-RL: The contour curve for the Signal-RL task lies much lower and is shifted to the right compared to the NLP-SL task. Moreover, the contour curve for Signal-RL is more ragged and fits well to an exponential curve that starts at $(0, 0)$ and intersects the line $p = 1$.
2. NLP-SL: The contour line for the NLP-SL task is smoother and fits well to a logistic function. When p in range $[0, 0.4]$, the decision boundary is relatively stable and remains around $q = 0.68$. For p in range $[0.4, 1.0]$, the contour line transitions into a sigmoid curve, with its midpoint around $p = 0.7$. This gradual transition reflects the trade-off between recovering critical information through accurate imputation and introducing ambiguities (e.g., incorrect word predictions) through noisy imputation.

The sigmoid shape of the NLP-SL contour line reflects a smoother transition between advantageous and disadvantageous regions as imputation noise increases, whereas the Signal-RL task exhibits an exponential drop-off in performance due to the compounding effect of errors in sequential decision-making. We classify tasks based on their sensitivity to noise:

- Noise-sensitive tasks: Tasks with contour curves below the diagonal (e.g., Signal-RL) are highly sensitive to noise, showing sharp performance degradation as imputation noise increases.
- Noise-insensitive tasks: Tasks with contour curves above the diagonal (e.g., NLP-SL) are more robust to imputation noise.

These observations are summarized in the Figure 9.

We also experimented with other common imputation methods. For NLP-SL, we designed two imputation methods: “wordvec” and “BERT.” The wordvec imputation method uses context word

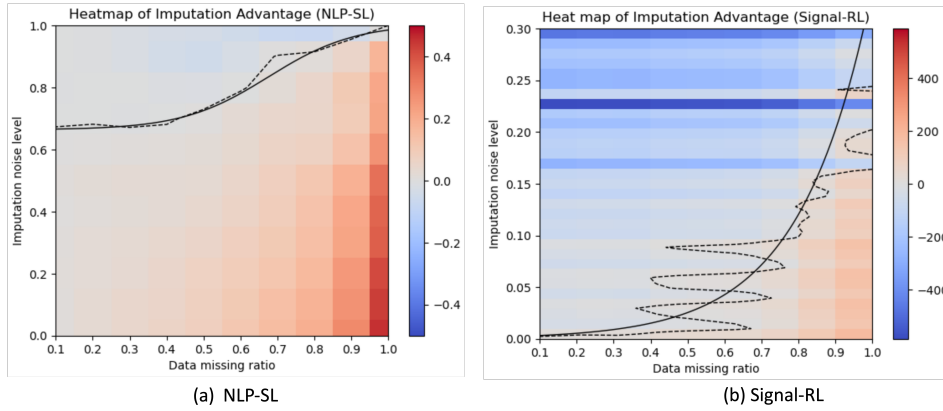


Figure 8: Heatmap of imputation advantage; x-axis is corruption ratio p and y-axis is imputation noise level q . (a) NLP-SL experiment; (b) Signal-RL experiment.

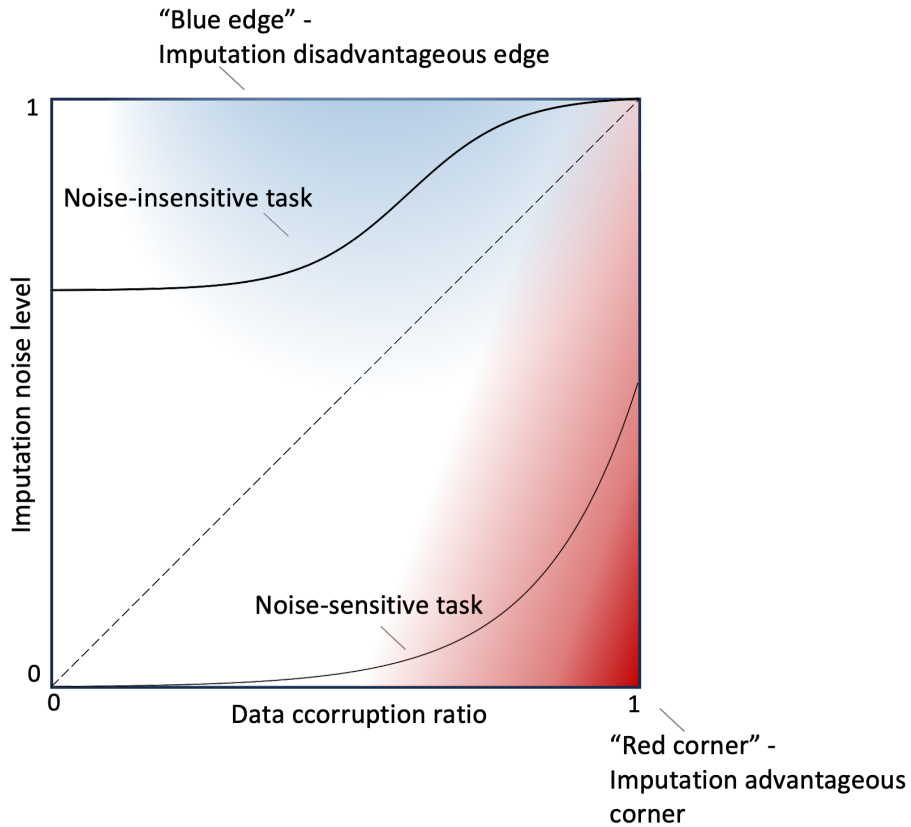


Figure 9: Illustration of imputation advantage pattern. "Red corner" and "blue edge" are areas where imputation advantage and disadvantage concentrate respectively. Task with decision boundary below diagonal line is called "noise-sensitive" and its decision boundary is exponential function shaped. Task with decision boundary above diagonal line is called "noise-insensitive" and its decision boundary is Logistic function shaped.

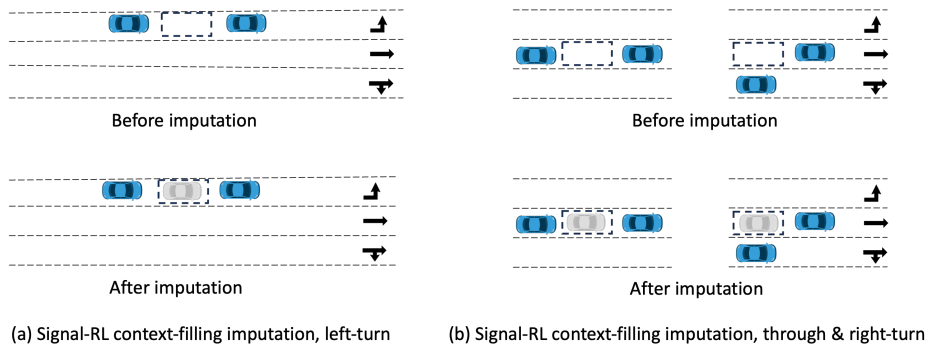


Figure 10: Illustration of context-filling imputation for Signal-RL experiment.

vector embeddings (e.g., GloVe) and cosine similarity to impute missing words. The BERT method leverages the pre-trained `bert-base-uncased` model for imputation. The results of these experiments are shown in Figure 11 (a) and (b). To speed up preprocessing, a subset ratio of `subset_ratio = 0.1` was used for BERT imputation.

The results indicate that BERT imputation improves the model score, whereas the wordvec method actually harms performance, suggesting that the wordvec approach introduces more noise than it resolves. An important observation is that common imputation methods do not maintain a fixed accuracy level as the missing data ratio p varies. Instead, their performance corresponds to curves, rather than horizontal lines, on the advantage heatmap.

For Signal-RL tasks, we designed an imputation method called “context-filling.” In this method, road occupancy cells with a value of zero are imputed as having a value of one if there are enough vehicles surrounding them, as illustrated in Figure 10. The model scores with context-filling imputation compared to no-imputation are shown in Figure 11. The results demonstrate that context-filling imputation introduces more harm than benefits for this noise-sensitive task.

The findings in this section provide valuable insights for making practical decisions about data imputation strategies. Specifically, they highlight the importance of tailoring imputation methods to the nature of the task and the type of data corruption present.

5 Effectiveness of Enlarging Dataset

Experiment Design

The aim of this section is to evaluate the effectiveness of enlarging the dataset and to quantify how much additional data is needed to offset the effects of data corruption. For the NLP-SL experiment, we recorded the performance of the model trained on datasets of different sizes and varying data corruption ratios. The variable “subset ratio” represents the proportion of the GLUE dataset used for fine-tuning. The results are shown in Figure 12 (a). For the Signal-RL task, we conducted experiments with different numbers of training episodes and data-missing ratios, as shown in Figure 12 (b).

Observations

As shown in the figure, as the dataset size increases, model performance converges. However, we observe that data corruption leads to a decline in model performance that cannot be fully recovered by increasing the sample size. When p is in the range $[0, 0.4]$, the performance decline is nearly linear with respect to p (Figure 12 (a)). For larger p , the model’s performance drops sharply to near zero (Figure 4).

This behavior is characteristic of an exponential function: for $e^x = 1 + x + \dots$, the linear term dominates when x is small. Hence, we conclude that the performance drop increases approximately exponentially as the data corruption ratio increases. In addition, data corruption also hampers learning efficiency. To achieve the same level of performance (if achievable at all for a corrupted model), the number of samples—and therefore the training time—required increases exponentially with the data corruption level. This is illustrated by the dashed benchmark line in Figure 12 (b). Quantitative curves showing the relationship between data quality and the required amount of clean data provide practical insights into data collection strategies. Code and detailed results of this study are shared at

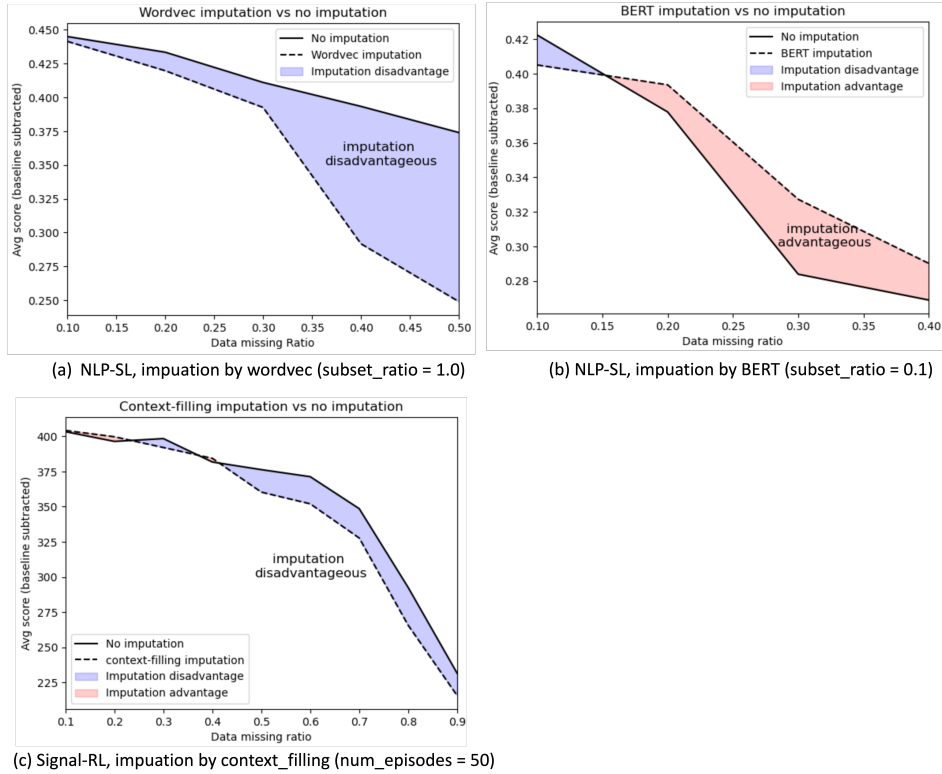


Figure 11: Effectiveness of other imputation methods.

[Github repository.](#)

6 Conclusions

In this paper, we explored the impact of data corruption, including missing and noisy data, on deep learning performance across two distinct domains: supervised learning with NLP tasks (NLP-SL) and deep reinforcement learning for traffic signal optimization (Signal-RL). Our experiments aimed to provide insights into the relationship between data quality and model performance, the trade-offs of imputation strategies, and the effectiveness of increasing data quantity as a remedy for data corruption.

Key Findings

1. **Diminishing Returns of Data Quality Improvement:** Both NLP-SL and Signal-RL experiments revealed that model performance follows a diminishing return curve as data corruption decreases. The relationship is well-modeled by the exponential function $S = a(1 - e^{-b(1-p)})$, highlighting that additional clean data yields less utility once most patterns are recovered. This universal trend emphasizes the importance of balancing data quality and preprocessing efforts.
2. **Noise vs. Missing Data:** Our results demonstrate that noisy data is significantly more detrimental than missing data, leading to faster performance degradation and increased training instability. This was particularly evident in the Signal-RL task, where inserting noise caused substantial fluctuations in both training and final policy stability.
3. **Imputation Trade-Offs:** Imputation methods can restore critical information for missing data but introduce a trade-off by potentially adding noise. The decision to impute depends on the imputation accuracy and the corruption ratio. The “imputation advantage heatmap” revealed two regions: a “red corner” where accurate imputation significantly improves performance and a “blue edge” where noisy imputation harms the model. Tasks were categorized as “noise-sensitive” or “noise-insensitive” based on their decision boundaries, with RL tasks exhibiting greater sensitivity due to the compounding effects of sequential decision-making.

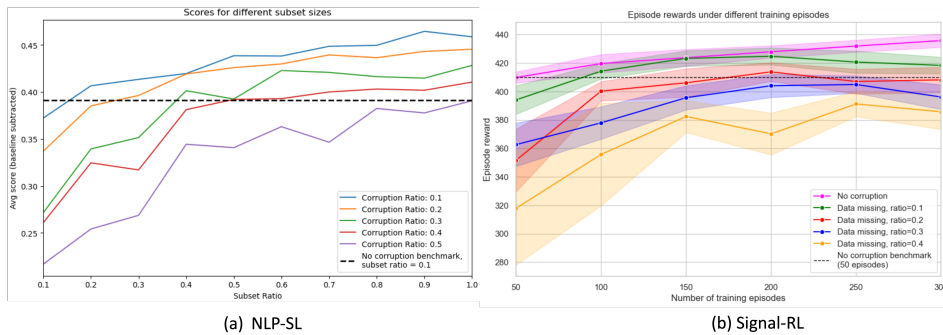


Figure 12: Effectiveness of enlarging training dataset. (a) NLP-SL (b) Signal-RL. data corruption leads to a decline in model performance, which cannot be fully recovered by increasing the sample size. To achieve the same level of performance (if achievable by the corrupted model), the number of samples, and hence the training time, required increases exponentially with the data corruption level.

4. Enlarging Dataset as a Remedy: Increasing the dataset size partially mitigates the effects of data corruption but cannot fully recover the lost performance, especially under high noise levels. The analysis showed that the number of samples required to achieve a certain performance level increases exponentially with the corruption ratio, confirming the exponential nature of the trade-off between data quality and quantity.
5. Empirical Rule for Critical Data: An empirical rule emerged from the experiments: approximately 30% of the data is critical for determining the model’s performance, while the remaining 70% can be lost without substantial impact. This observation provides practical guidance for prioritizing efforts in data collection and preprocessing.

Implications

Our findings offer valuable insights for machine learning practitioners and researchers. In resource-constrained environments, focusing on improving data quality for a small, critical portion of the dataset may yield higher returns than attempting to clean all data. Additionally, understanding the trade-offs of imputation strategies can inform the choice of preprocessing methods based on task sensitivity and corruption characteristics. For RL tasks, where noise compounds over sequential decisions, more robust strategies to handle corrupted observations are critical.

Future Work

This study opens up several avenues for future research. First, the observed patterns and empirical rules should be validated across broader datasets and additional machine learning tasks, such as computer vision and time-series forecasting. Second, developing adaptive imputation strategies that dynamically balance missing data recovery and noise introduction could further enhance model robustness. Finally, theoretical work on the relationship between information entropy, marginal utility, and model learning dynamics under corrupted data could deepen our understanding of these phenomena.

By addressing these challenges, we hope to advance the field’s ability to build robust machine learning models that perform reliably even in the presence of real-world data corruption.

References

- [BFOS84] Leo Breiman, Jerome H. Friedman, Richard A. Olshen, and Charles J. Stone. *Classification and Regression Trees*. Wadsworth International Group, Belmont, CA, 1984.
- [BGW19] Xueying Bai, Jian Guan, and Hongning Wang. A model-based reinforcement learning with adversarial training for online recommendation. *Advances in Neural Information Processing Systems*, 32, 2019.
- [Bre01] Leo Breiman. Random forests. *Machine Learning*, 45(1):5–32, 2001.
- [Bro20] Tom B Brown. Language models are few-shot learners. *arXiv preprint arXiv:2005.14165*, 2020.

- [CPC⁺18] Zhengping Che, Sanjay Purushotham, Kyunghyun Cho, David Sontag, and Yan Liu. Recurrent neural networks for multivariate time series with missing values. *Scientific reports*, 8(1):6085, 2018.
- [Dev18] Jacob Devlin. Bert: Pre-training of deep bidirectional transformers for language understanding. *arXiv preprint arXiv:1810.04805*, 2018.
- [GGS⁺20] Samuel Gehman, Suchin Gururangan, Maarten Sap, Yejin Choi, and Noah A Smith. Realtotoxicityprompts: Evaluating neural toxic degeneration in language models. *arXiv preprint arXiv:2009.11462*, 2020.
- [GPAM⁺14] Ian Goodfellow, Jean Pouget-Abadie, Mehdi Mirza, Bing Xu, David Warde-Farley, Sherjil Ozair, Aaron Courville, and Yoshua Bengio. Generative adversarial nets. In *Advances in Neural Information Processing Systems*, volume 27, pages 2672–2680, 2014.
- [HS15] Matthew Hausknecht and Peter Stone. Deep recurrent q-learning for partially observable mdps. In *2015 aaai fall symposium series*, 2015.
- [JCL⁺20] Mandar Joshi, Danqi Chen, Yinhan Liu, Daniel S Weld, Luke Zettlemoyer, and Omer Levy. Spanbert: Improving pre-training by representing and predicting spans. *Transactions of the association for computational linguistics*, 8:64–77, 2020.
- [Liu19] Yinhan Liu. Roberta: A robustly optimized bert pretraining approach. *arXiv preprint arXiv:1907.11692*, 364, 2019.
- [MKS⁺15] Volodymyr Mnih, Koray Kavukcuoglu, David Silver, Andrei A Rusu, Joel Veness, Marc G Bellemare, Alex Graves, Martin Riedmiller, Andreas K Fidjeland, Georg Ostrovski, et al. Human-level control through deep reinforcement learning. *nature*, 518(7540):529–533, 2015.
- [PAED17] Deepak Pathak, Pulkit Agrawal, Alexei A Efros, and Trevor Darrell. Curiosity-driven exploration by self-supervised prediction. In *International conference on machine learning*, pages 2778–2787. PMLR, 2017.
- [PPF⁺20] Fabio Petroni, Aleksandra Piktus, Angela Fan, Patrick Lewis, Majid Yazdani, Nicola De Cao, James Thorne, Yacine Jernite, Vladimir Karpukhin, Jean Maillard, et al. Kilt: a benchmark for knowledge intensive language tasks. *arXiv preprint arXiv:2009.02252*, 2020.
- [Rub76] Donald B. Rubin. Inference and missing data. *Biometrika*, 63(3):581–592, 1976.
- [Rub87] Donald B. Rubin. *Multiple Imputation for Nonresponse in Surveys*. Wiley, New York, 1987.
- [SG02] Joseph L. Schafer and John W. Graham. Missing data: Our view of the state of the art. *Psychological Methods*, 7(2):147–177, 2002.
- [TCS⁺01] Olga Troyanskaya, Michael Cantor, Gavin Sherlock, Pat Brown, Trevor Hastie, Robert Tibshirani, David Botstein, and Russ B. Altman. Missing value estimation methods for DNA microarrays. *Bioinformatics*, 17(6):520–525, 2001.
- [THBM19] Wang Tong, Azhar Hussain, Wang Xi Bo, and Sabita Maharjan. Artificial intelligence for vehicle-to-everything: A survey. *IEEE Access*, 7:10823–10843, 2019.
- [TS09] Matthew E Taylor and Peter Stone. Transfer learning for reinforcement learning domains: A survey. *Journal of Machine Learning Research*, 10(7), 2009.
- [VLBM08] Pascal Vincent, Hugo Larochelle, Yoshua Bengio, and Pierre-Antoine Manzagol. Extracting and composing robust features with denoising autoencoders. In *Proceedings of the 25th International Conference on Machine Learning*, pages 1096–1103, 2008.
- [YWZ21] Jieyuan Yuan, Rui Wang, and Yue Zhang. Missing token imputation using masked language models. In *Proceedings of the 2021 Conference on Empirical Methods in Natural Language Processing*, pages 1234–1240, 2021.